Title

In vivo 1H MRS of human gallbladder bile at 3 T in one and two dimensions: detection and quantification of major biliary lipids

Journal

NMR in Biomedicine, 27(10)

ISSN

0952-3480

Authors

Mohajeri, Sanaz
Ijare, Omkar B
Bezabeh, Tedros
et al.

Publication Date

2014-10-01

DOI

10.1002/nbm.3173

Peer reviewed

Research article

NMR IN BIOMEDICINE

Received: 06 January 2014, Revised: 29 June 2014, Accepted: 30 June 2014, Published online in Wiley Online Library: 14 August 2014

(wileyonlinelibrary.com) DOI: 10.1002/nbm.3173

In vivo ^{1}H MRS of human gallbladder bile at 3 T in one and two dimensions: detection and quantification of major biliary lipids†

Sanaz Mohajeri[a], Omkar B. Ijare[b], Tedros Bezabeh[a,b]*, Scott B. King[c], M. Albert Thomas[d], Gerald Minuk[a], Jeremy Lipschitz[a], Iain Kirkpatrick[a], Mike Smith[c] and Ian C. P. Smith[a,b]

In vitro **^{1}H MRS of human bile has shown potential in the diagnosis of various hepatopancreatobiliary (HPB) diseases. Previously, *in vivo* ^{1}H MRS of human bile in gallbladder using a 1.5 T scanner demonstrated the possibility of quantification of choline-containing phospholipids (chol-PLs). However, other lipid components such as bile acids play an important role in the pathophysiology of the HPB system. We have employed a higher magnetic field strength (3 T), and a custom-built receive array coil, to improve the quality of *in vivo* ^{1}H MRS of human bile in the gallbladder. We obtained significant improvement in the quality of 1D spectra (17 healthy volunteers) using a respiratory-gated PRESS sequence with well distinguished signals for total bile acids (TBAs) plus cholesterol resonating at 0.66 ppm, taurine-conjugated bile acids (TCBAs) at 3.08 ppm, chol-PLs at 3.22 ppm, glycine-conjugated bile acids (GCBAs) at 3.74 ppm, and the amide proton (−NH) arising from GCBAs and TCBAs in the region 7.76–8.05 ppm. The peak areas of these signals were measured by deconvolution, and subsequently the molar concentrations of metabolites were estimated with good accuracy, except for that of TBAs plus cholesterol. The concentration of TBAs plus cholesterol was overestimated in some cases, which could be due to lipid contamination. In addition, we report the first 2D L-COSY spectra of human gallbladder bile *in vivo* (obtained in 15 healthy volunteers). 2D L-COSY spectra will be helpful in differentiating various biliary chol-PLs in pathological conditions of the HPB system. Copyright © 2014 John Wiley & Sons, Ltd.**

Keywords: human bile; *in vivo* ^{1}H MRS; glycine-conjugated bile acids; taurine-conjugated bile acids; choline-containing phospholipids; PRESS; L-COSY

INTRODUCTION

Bile is a yellowish green fluid secreted by liver, stored and concentrated in the gallbladder and released to the duodenum in response to cholecystokinin following ingestion of food (1). It is mainly composed of water, pigments such as bilirubin, lipids including choline-containing phospholipids (chol-PLs), cholesterol, and bile salts such as glycine-conjugated bile acids (GCBAs) and taurine-conjugated bile acids (TCBAs) (2–4). Bile salts play a major role in emulsification, digestion, and absorption of lipids. Moreover, the common bile duct receives pancreatic secretions through the pancreatic duct before emptying to the duodenum (2). Therefore, the metabolic profile of bile delivered to the intestine is mainly under the control of cellular secretions of liver, gallbladder, pancreas, and bile ducts. As a result, any pathological changes in the gastrointestinal system, especially the hepatopancreatobiliary (HPB) part, can affect the metabolic profile of the bile (1–4). Among these metabolites, cholesterol, chol-PLs, and bile acids have captured more attention, due to their higher concentration and greater role in the disease processes (4–8).

Various *in vitro* studies have demonstrated the potential of MRS in the diagnosis of HPB pathologies, especially in differentiating benign changes from malignant ones through analysis of chol-PLs, bile acids, and cholesterol in the bile (4,6,7,9). The recent success from our laboratory in the simultaneous quantification of bile acids

* *Correspondence to: T. Bezabeh, Chemistry, University of Winnipeg, Winnipeg, Manitoba, Canada R3B 2E9*
E-mail: t.bezabeh@uwinnipeg.ca

† *This work was partially presented at the International Society of Magnetic Resonance in Medicine Annual Meeting, Montreal, 2011.*

a *S. Mohajeri, T. Bezabeh, G. Minuk, J. Lipschitz, I. Kirkpatrick, I. C. P. Smith*
University of Manitoba, Winnipeg, Manitoba, Canada

b *O. B. Ijare, T. Bezabeh, I. C. P. Smith*
University of Winnipeg, Winnipeg, Manitoba, Canada

c *S. B. King, M. Smith*
National Research Council of Canada, Winnipeg, Manitoba, Canada

d *M. A. Thomas*
University of California, Los Angeles, CA, USA

Abbreviations used: *ALP, alkaline phosphatase; ALT, alanine aminotransferase; AST, aspartate aminotransferase; chol-PLs, choline-containing phospholipids; DSS, 3-(trimethylsilyl)-1-propanesulfonic acid sodium salt; ERCP, endoscopic retrograde cholangiopancreatography; FID, free induction decay; GCBAs, glycine-conjugated bile acids; GDCA, glycodeoxycholic acid sodium salt; GGT, gamma-glutamyl transferase; HASTE, half-Fourier acquisition single-shot turbo spin-echo; HPB, hepatopancreatobiliary; INR, international normalized ratio; PC, phosphatidylcholine; PhC, phosphocholine chloride calcium salt tetrahydrate; TBAs, total bile acids; TCA, taurocholic acid sodium salt; TCBAs, taurine-conjugated bile acids; T_{Reff}, effective T_R.*

(GCBAs, TCBAs, and total bile acids, TBAs), along with the chol-PLs, is an important development in the application of *in vitro* ^{1}H MRS of bile (10). This progress has generated hope for following the metabolic footprints of different HPB disorders (10). Moreover, analyzing the ratio of concentrations of metabolites can also provide additional diagnostic information. For example, in our previous study (11) comparing cholestatic hyperbilirubinemic hepatobiliary patients with normobilirubinemic cases, the ratio of biliary GCBAs to TCBAs was found to decrease by an amount that was statistically significant. However, the changes in the concentrations of the individual GCBAs and TCBAs were not statistically significant.

Analysis of bile spectra has its own difficulties. The similarities in the structures of constituent bile acids in bile may result in significant overlap of peaks of interest, especially in *in vivo* MRS studies. To overcome such difficulties, different NMR methods have been developed (12,13). Spectral editing MRS sequences may overcome this problem (14), but they can only measure one metabolite at a time. However, 2D MRS techniques such as COSY may virtually separate multiple overlapping peaks in a single measurement, providing unambiguous assignment. Therefore, they may become the techniques of choice in such cases (15,16).

For years, providing metabolic information using MRS non-invasively was difficult, primarily due to the complexities of *in vivo* MRS. The challenges include overlapping of metabolite peaks due to the use of lower magnetic field strengths (typically 1.5 T, compared with 9.4–14.1 T for *in vitro* studies), magnetic susceptibility effects, and motion artifacts (17). Advances in MR technology, at the levels of both hardware and software, have decreased such bottlenecks to a large extent. The increase in magnetic field strength of clinical scanners (≥3 T), and the development of gated sequences (to minimize the effect of motion artifacts), has been quite helpful. As a result, there has been a great interest in the detection and quantification of bile metabolites with diagnostic potential using *in vivo* ^{1}H MRS (18,19). Prescot *et al.* performed the first *in vivo* ^{1}H MRS study on human gallbladder bile, using a 1.5 T MRI scanner and a surface coil in receive mode (18). However, the published *in vivo* spectra were of low quality, and the authors were unable to quantify individual bile components other than chol-PLs. This could be due to the lower magnetic field strength (1.5 T), use of a spin echo sequence with long delays (T_E = 60 ms), and/or lipid contamination (18). Künnecke *et al.* were successful in obtaining a better quality spectrum of bile *in vivo* in cynomolgus monkeys using a 4.7 T animal scanner and a custom-built surface coil in transmit–receive mode with the aid of a respiratory-gated sequence (19). They identified and quantified different bile components, bile acids, and their taurine and glycine conjugates, including the previously reported chol-PLs (19).

Our preliminary study on pigs using a 3 T clinical scanner and a custom-built receive array coil revealed a significant improvement in the quality of *in vivo* ^{1}H spectra of gallbladder bile (20,21). The resultant spectra were promising enough to recommend exploring the possibility of acquiring such spectra in humans. In the current study, we report 1D ^{1}H MRS of human gallbladder bile at 3 T, including the detection and quantification of major lipid components. In addition, we report the first acquisition of 2D L-COSY data for human gallbladder bile *in vivo*.

METHODS

Subject characteristics

Healthy volunteers were recruited at the National Research Council (NRC) and Health Sciences Centre, University of Manitoba, Winnipeg, according to the protocol approved by the Research Ethics Boards of the University of Manitoba and the NRC. Informed consent was obtained from each subject and the study protocol conforms to the ethical guidelines of the 1975 Declaration of Helsinki. The subjects had no history of acute or chronic liver disease, inflammatory bowel disease or heavy alcohol use (>3 drinks/day). None of the subjects was on medication that could cause liver toxicity. The possibility of active HPB disorders was ruled out in all subjects using a combination of medical history, physical examination, and laboratory blood tests including bilirubin (total and direct), aspartate aminotransferase (AST), alanine aminotransferase (ALT), gamma-glutamyl transferase (GGT), lipase, alkaline phosphatase (ALP), and international normalized ratio (INR).

After optimizing the scanning parameters on a number of healthy volunteers, MRS data were acquired from 22 subjects. We collected 1D data from 17/22 subjects and 2D data from 15/22 subjects. We were able to acquire both 1D and 2D data in 7/22 subjects. Out of the 17 1D spectra, 3 were excluded due to lipid contamination, ineffective water suppression, or motion artifacts due to failed respiratory gating. The 14 subjects included in the final 1D analysis comprised 11 females and 3 males (mean ages 40 and 33 respectively, range 21–55). In the case of 2D, data from 4/15 subjects were excluded due to low SNR and the same issues described above. The 11 subjects included in the final 2D analysis were 7 females and 4 males (mean ages 41 and 35 respectively, range 26–55). Details of the subjects' characteristics and biochemical data are given in Table 1.

MRS experiments

MRS experiments were performed on a Siemens 3 T Magnetom Trio clinical scanner (RF transmitter frequency = 123.22 MHz). The body coil transmitted the RF pulses. A custom-built surface receive array coil, which passed the safety checks of the NRC and was approved by the research ethics boards of both the NRC and the University of Manitoba, was used as an RF receiver. Single voxel spectroscopy was performed using the PRESS sequence with bellow respiratory gating (VB15 and VB17, Siemens, Erlangen, Germany). 1D experiments were performed on solutions of phosphocholine chloride calcium salt tetrahydrate (PhC), taurocholic acid sodium salt (TCA), and glycodeoxycholic acid sodium salt (GDCA), representing three major biliary biochemicals – chol-PLs, TCBAs, and GCBAs, respectively. These experiments were used to verify the accuracy of quantification of chol-PLs, TCBAs, and GCBAs in the bile at 3 T. The 1D ^{1}H spectra were then acquired from human gallbladder bile *in vivo*. Finally, we edited the PRESS sequence to L-COSY as described by Thomas *et al.* (15). In this method, the last 180° refocusing pulse of the PRESS sequence was replaced by a hyperbolic secant 90°, the same as the first 90° excitation RF pulse, and a 0.8 ms time increment (Δt_1) was applied between the first refocusing and the second 90° (coherence transfer) RF pulse in each measurement (15). In both 1D and 2D experiments, we optimized the voxel size to $12 \times 12 \times 12$ mm^3 to minimize the effect of lipid contamination from the liver or the body fat outside the gallbladder. Spatial saturation bands were positioned around the gallbladder in order to further minimize such effects. Application of bellow respiratory-gated sequences reduced the extent of motion artifact due to breathing. With manual shimming, we achieved a full width half-maximum of less than 15 Hz. The bandwidth of the water suppression pulses was adjusted to 35 Hz on

Table 1. Age, sex, and blood biochemistry of healthy volunteers participating in the study

Subject	Age	Sex	Bilirubin total (μM)	Bilirubin direct (μM)	AST (U/L)	ALT (U/L)	GGT (U/L)	Lipase (U/L)	ALP (U/L)	INR
1	41	F	9	3	22	14	—	69	77	—
2	43	M	5	2	21	19	—	40	69	1.2
3	21	F	7	—	19	20	—	31	74	0.9
4*	26	F	6	<2	17	15	13	30	41	1
5*	36	F	20	4	22	13	22	35	51	—
6*	54	F	8	2	23	14	18	30	84	1
7*	27	M	—	5	31	24	14	20	80	1
8	55	F	3	<2	22	20	—	44	86	1.1
9	31	F	4	<2	19	17	—	84	50	1
10	44	F	10	<2	20	12	11	41	43	1
11*	26	F	13	3	19	14	14	35	50	1
12	49	F	4	<2	20	15	14	50	59	0.9
13*	54	F	6	<2	20	17	10	—	73	0.9
14*	29	M	15	3	35	17	13	46	71	1
15#	36	M	9	2	19	21	—	45	102	1
16#	49	M	3	<2	22	43	37	39	72	1
17#	55	F	4	<2	24	15	20	45	75	1
18#	38	F	8	<2	26	33	35	23	55	0.9

—, not reported by the clinical laboratory; *, participated in both 1D and 2D experiments; #, participated only in 2D experiments. μM, micromolar; U/L, unit/liter; M, male; F, female.
Normal values of blood biochemistry: bilirubin total, 2–20 μM; bilirubin direct, <7 μM; AST, 10–32 U/L; ALT, M, <30, F, <25 U/L; GGT, M, 5–38, F, 5–29 U/L; lipase, <60 U/L; ALP, 30–120 U/L; INR, 0.9–1.1.

VB15. There were some changes in the water suppression code on VB 17, and as a result we increased the bandwidth from 35 to 50 Hz to obtain water suppression quality comparable to that on VB15. The increase in bandwidth did not affect any of the peaks of interest.

One-dimensional ^{1}H MR experiments

In vitro phantom measurements

Aqueous solutions of PhC, TCA, and GDCA, representing the major bile components (chol-PLs, TCBAs, and GCBAs), were prepared based on a method described in the LCModel User's Manual (22). Each phantom contained a solution of a metabolite with known concentration (21.24 mM PhC, 20.18 mM TCA, or 37.42 mM GDCA), 210 mM sodium formate, and 2.0 mM 3-(trimethylsilyl)-1-propanesulfonic acid sodium salt (DSS). The pH of all the phantom solutions was adjusted to 7.2 using 1.0 M hydrochloric acid/sodium hydroxide. The above solutions of each metabolite were held in a sealed container, which was immersed in a water container (by gluing it to the bottom) surrounded by an oil container resembling the fat around the gallbladder.

Three orthogonal MR images were acquired using half-Fourier acquisition single-shot turbo spin-echo (HASTE) sequences (VB15 and VB17, Siemens) (matrix = 192 × 256, slice thickness = 6 mm, FOV = 270 × 360 mm^2, T_E/T_R =101/1000 ms) in order to localize the solution container. Six spatial saturation bands were placed around the water container in order to minimize the effect of the surrounding oil. After adjusting the frequency and the receiver gain, manual shimming and water suppression were performed. 1D ^{1}H spectra were acquired from the above three solutions using the PRESS sequence. The following acquisition parameters were used: voxel size = 12 × 12 × 12 mm^3, T_E = 30 ms, T_R = 10000 ms, bandwidth = 2000 Hz, vector size 2048 points, and N_S = 256. A second spectrum with eight scans was acquired from the same voxel using the same parameters but without water suppression in each experiment.

In vivo measurements

The subjects fasted for at least 4 h before the study. Three orthogonal MR images were used to localize the gallbladder. The images were obtained during breath hold at the end of a regular expiration using HASTE sequences with acquisition parameters identical to those mentioned above. A 12 × 12 × 12 mm^3 voxel was positioned in the gallbladder using these images. Six spatial saturation bands were positioned around the gallbladder in order to reduce lipid contamination. After adjusting the frequency and setting the receiver gain to high, manual shimming and water suppression were performed. 1D spectra were obtained using the bellow respiratory-gated PRESS sequence during the last 10–30% of quiet expiration. The acquisition parameters were the same as those of *in vitro* experiments except for T_R, which was 2000 ms. We used the minimum possible T_E (=30 ms) of the Siemens instrument in order to reduce signal loss due to T_2 relaxation. Although the T_R was 2000 ms, one free induction decay (FID) was recorded in each breath. Therefore, the effective T_R (T_{Reff}) was considered to be equal to the average breathing cycle length in each subject. Considering that the scanning time obtained for each sequence from the scanner includes the adjustment time, we could not use the water suppressed 1D or 2D spectra to calculate T_{Reff}. Since the unsuppressed water 1D spectrum was acquired immediately after the 1D spectrum with

the same parameters (no need for adjustments), we used these data for calculating T_{Reff}. We divided the scanning time by the number of scans to calculate the average breathing cycle length, which was equal to T_{Reff}. As a result, the T_{Reff} in different subjects was variable in the range of 3750–7438 ms, and the mean of T_{Reff} in all subjects was 5366 ms. Therefore, our spectra in most cases were almost fully relaxed. N_S was 256 except in one case, which was 128. The average time for gallbladder localization, adjustment of parameters, and data acquisition was 42 min. Considering that the average T_{Reff} was 5366 ms, the average time for 256 scans was 22.89 min. The rest of the time was needed for acquiring localizer images, manual adjustments (specially shimming and water suppression), and acquiring the 1D spectrum with unsuppressed water.

Two-dimensional *in vivo* ^{1}H MR experiments

Although it is possible to identify and quantify different metabolites using 1D ^{1}H MRS, the presence of overlapping signals from structurally similar metabolites makes the identification of some of the resonances very challenging. Therefore, we made use of 2D L-COSY experiments to detect some of these signals unambiguously (15,16). A $12 \times 12 \times 12\ mm^3$ voxel was positioned in the gallbladder using the three orthogonal localizer images. Spatial saturation bands were positioned around the gallbladder to reduce lipid contamination. After adjusting the frequency, and setting the receiver gain to high, manual shimming and water suppression were performed. 2D L-COSY data were acquired during the last 10–30% of quiet expiration using the bellow respiratory-gated sequence. The following spectral parameters were used throughout: $T_E = 30$ ms, $T_R = 2000$ ms, bandwidth = 2000 Hz, vector size = 2048 points, $N_S = 12$, time increment (Δt_1) = 0.8 ms, and number of measurements = 50 or 64 except in one case, which had only 40 measurements. The original minimum T_R was set to 2000 ms. Considering that in each breath one FID was recorded, the T_{Reff} was variable. The approximate time for adjusting parameters and the collection of 2D data was 49 min. In the majority of cases, since the 2D data were acquired right after 1D, there was no need to repeat the localizers and we used the adjusted parameters from 1D as a guideline and performed only fine adjustments (which took a very short time). As a result, if we ignore the adjustment time, the average T_{Reff} for 2D will be 4548 ms, which is shorter than that for 1D. The maximum T_1 relaxation time for our metabolites of interest presented in Table 2 is 383 ms (for TCBAs). If we have $T_R > 5\,T_1$ ($5 \times 383 = 1915$ ms), then the spectrum will be fully relaxed. The range of T_{Reff} for 2D experiments was 3672–5700 ms. Moreover, by choosing the minimum possible T_R of 2000 ms, we made sure that the variation in T_{Reff} did not affect the qualitative analysis of the 2D data.

Data processing

1D ^{1}H MR experiments

The raw data (.meas files from the Siemens scanner) were first processed by an in-house MATLAB program generated at UCLA (Dr Thomas's laboratory), and modified at NRC. This program facilitated the inspection of individual scans. The scans which were distorted by lipid contamination, failed water suppression or with very low SNR (no detectable signal) were discarded. Out of the 256 scans acquired, 216 undistorted scans were averaged in all subjects except for two cases. In the first case, only 128 scans were acquired due to time limitation. Out of 128 scans, 119 were analyzed after eliminating the distorted scans. In the other case, out of 256 scans only 52 were analyzed. The individual spectra in all scans were aligned (using the methylene ($-CH_2-$) proton signal of the lipid peak at 1.26 ppm or the trimethylammonium ($-N^+(CH_3)_3$) signal of chol-PLs at 3.22 ppm) to minimize frequency drifts due to breathing motion artifacts, and then averaged. Eddy current correction was applied using the unsuppressed water signal (23) and the data from individual coil elements were combined using an optimized method based on noise correlation (24). After this preliminary processing, the data were transferred to FELIX-2007 software (FELIX NMR, San Diego, CA, USA). The data were then apodized using an exponential function with a line broadening of 0.5 Hz, and Fourier transformed. First and second order phase and baseline corrections were applied on the real part of the spectrum. Finally, the spectrum was referenced to the lipid $-CH_2-$ peak at 1.26 ppm or the $-N^+(CH_3)_3$ signal of chol-PLs at 3.22 ppm. The data acquired from phantom solutions were processed similarly. The first 216 scans were averaged and the spectrum was referenced to the DSS signal at 0 ppm.

Quantification of biliary biochemicals

Chemical shift assignments in the bile ^{1}H spectrum were made according to the previous *in vitro* (10,12) and *in vivo* studies on human (18) and monkey bile (19). Twenty-one different peaks in the water-suppressed bile ^{1}H spectrum were fitted to Lorentzian line shapes by deconvolution based on a simulated annealing algorithm (FELIX NMR). Similarly, the water peak of the bile spectrum obtained without water suppression was fitted and used as an internal reference. After fitting, the peak areas of the methyl ($-CH_3$) signal representing TBAs plus cholesterol at 0.66 ppm, the $-CH_2-$ signal of TCBAs at 3.08 ppm, the $-N^+(CH_3)_3$ signal of chol-PLs at 3.22 ppm, the $-CH_2-$ signal of GCBAs at 3.74 ppm, and the amide signals ($-NH$) of GCBAs and TCBAs in the region 7.76–8.05 ppm were measured. Molar concentrations of all the above biliary lipids were calculated using the following equation, similar to that reported by Fayad *et al.* (25):

Table 2. T_1, T_2 relaxation times of major bile metabolites calculated using porcine bile

Metabolite	TBAs 0.65 ppm	TCBAs 3.01 ppm	chol-PLs 3.22 + 3.15 ppm*	GCBAs 3.74 ppm	GCBAs + TCBAs 7.95 ppm	Water 4.78 ppm
T_1 value (ms)	233	383	298	360	352	780
T_2 value (ms)	25	93	155	84	36	172

T_1 and T_2 relaxation times were calculated using FELIX 2007 software.
*, porcine bile used for T_1 and T_2 measurements showed an additional peak at 3.15 ppm in the chol-PL region.

$$[\text{lipid}]\ (\text{mM}) = \frac{\text{peak area(lipid)}}{\text{peak area(H2O)}} \cdot \frac{\text{No of protons(H2O)}}{\text{No of protons(lipid)}} \cdot \frac{10^6}{\text{mol. wt(H2O)}} \cdot \frac{fT1(\text{H2O})}{fT1(\text{lipid})} \cdot \frac{fT2(\text{H2O})}{fT2(\text{lipid})} \cdot \text{CF(H2O)} \quad [1]$$

where $CF(H_2O) = 0.9$ is a conversion factor for the water content of human gallbladder bile, which is considered to be 90% by weight (26), $fT_1 = 1 - \exp(-T_R/T_1)$ and $fT_2 = \exp(-T_E/T_2)$ are correction factors due to the T_1 and T_2 relaxation times of water and individual lipid molecules and were calculated as reported elsewhere (25,27) and presented in Table 2. In order to confirm the accuracy of the calculations, the peak areas of the signals acquired from phantom solutions were also quantified similarly.

2D L-COSY experiments

After preliminary processing with the MATLAB program as described for the 1D experiments, the 2D raw data were transferred to FELIX-2007 software (FELIX NMR), and processed in the magnitude mode. The first 256 points in the $\boldsymbol{t}_2$ dimension and the first 50 measurements in the $\boldsymbol{t}_1$ dimension were processed. In one case we just had 40 points to process in the $\boldsymbol{t}_1$ dimension because we acquired only 40 measurements. There was also another case where we were only able to process the first 39 measurements due to technical issues. The $\boldsymbol{t}_1$ dimension was linear predicted to 64 measurements. The raw data were zero filled to 2048 and 128 points along $\boldsymbol{t}_2$ and $\boldsymbol{t}_1$ dimensions respectively. In order to reduce noise, a skewed sine-bell apodization function with 0° shift (skew parameter of 0.5–0.6) was applied in both dimensions. After complex Fourier transformation in both dimensions, the spectra were referenced to the diagonal peak of chol-PLs ($F_2 = F_1 = 3.22$ ppm) or to the diagonal peak of the amide signal ($F_2 = F_1 = 7.81$ ppm).

RESULTS

Figure 1 represents the ^{1}H spectra of PhC, TCA and GDCA solutions representing three major biliary biochemicals – chol-PLs, TCBAs and GCBAs. The assignment of peaks and their selection for the quantification was based on the results from previous *in vitro* (10,12) and *in vivo* (18,19) studies. Figure 1(A) shows the ^{1}H MR spectrum of an aqueous solution of PhC. We used PhC instead of phosphatidylcholine (PC) due to the similarity of its head group with that of PC and also due to its free solubility in water. The peak at 3.20 ppm was assigned to the $-N^+(CH_3)_3$ group of PhC. Figure 1(B) was obtained from the phantom solution of TCA representing TCBAs. The triplet at 3.06 ppm is due to its H-26 $-CH_2-$ signal, whereas peaks at 0.68 and 7.99 ppm were assigned to the H-18 $-CH_3$ and amide (−NH) groups of TCBAs respectively. Figure 1(C) represents the spectrum recorded from a GDCA solution. The signals resonating at 0.68, 3.72 and 7.83 ppm were assigned to the H-18 $-CH_3$, the H-25 $-CH_2-$ and the amide (−NH) group of GCBAs respectively. All these spectra were recorded using a T_R of 10000 ms and T_E of 30 ms, ensuring complete relaxation and with negligible T_2 loss.

T_1 and T_2 relaxation times of various bile metabolites were measured using porcine bile. Table 2 lists the T_1 and T_2 values of major bile metabolites quantified in this study, including water, which was used as an internal reference. Table 3 lists actual and calculated concentrations of biochemicals from phantom solutions determined using current quantification methodology. The concentrations of metabolites before and after applying T_1 and T_2 corrections were compared with the actual concentration of each phantom solution to prove the reliability of the quantification. The concentrations of metabolites determined after applying both T_1 and T_2 corrections were very close to the actual concentrations, except for GCBAs, which were quantified using the amide (−NH) signal resonating at 7.83 ppm.

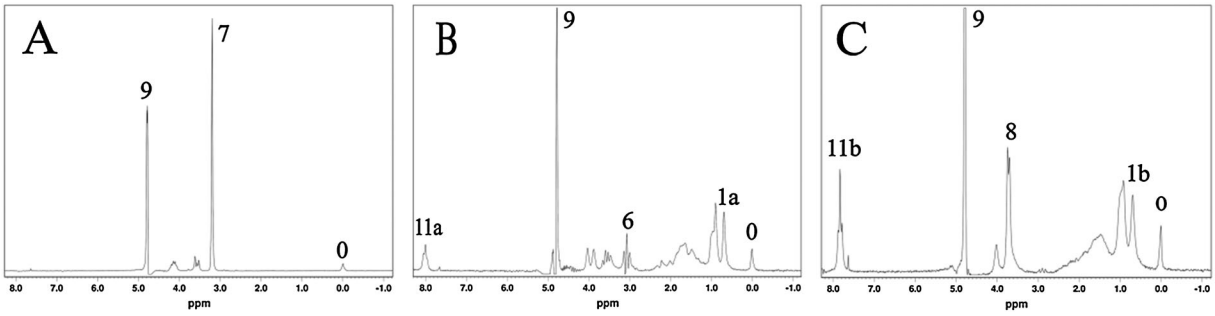

Figure 1. ^{1}H spectra of (A) PhC, (B) TCA and (C) GDCA solutions representing three major biliary biochemicals – chol-PLs, TCBAs and GCBAs respectively. The signals were assigned based on the previous *in vitro* (10,12) and *in vivo* studies (18,19). *Assignments:* 0, DSS; 7, $-N^+(CH_3)_3$ group of PhC; 9, residual water; 1a, H-18 protons of $-CH_3$ group of TCA; 6, H-26 protons of $-CH_2-$ group of TCA; 11a, amide (−NH) group of TCA; 1b, H-18 protons of $-CH_3$ group of GDCA; 8, H-25 protons of $-CH_2-$ group of GDCA; 11b, amide (−NH) group of GDCA.

Table 3. Concentration of metabolites (mM) before and after T_1 and T_2 corrections compared with the actual concentrations of phantom solutions

Metabolite (peak used)	PhC (3.20 ppm)	TCA (0.68 ppm)	TCA (7.99 ppm)	GDCA (0.68 ppm)	GDCA (3.72 ppm)	GDCA (7.83 ppm)
Concentration (mM)	22.69	7.08	11.26	13.74	32.41	37.04
Corrected concentration (mM)	23.13	19.74	21.77	38.31	38.90	71.59
Solution concentration (mM)	21.24	20.18	20.18	37.42	37.42	37.42

From Table 3, it is clear that no corrections were required for the quantification of GCBAs determined using their amide signal. Since the amide peak in human/porcine bile is a combination of both TCBAs and GCBAs, the T_1 and T_2 corrections are mainly required for the amide signal of TCBAs. Since the H-26 $-CH_2-$ signal of TCA at 3.06 ppm (peak 6 in Fig. 1(B)) had an apparent phasing problem, the quantification of this signal in the phantom experiments was not feasible.

Figure 2 illustrates a typical ^{1}H MR spectrum recorded from the gallbladder bile of a healthy volunteer *in vivo* at 3 T using a custom-built receive-only coil. Panels (A)–(C) represent three orthogonal images acquired at the end of expiration during a regular breath-hold in order to position a $12 \times 12 \times 12\ mm^3$ voxel in the gallbladder. Panel (D) shows the corresponding ^{1}H MR spectrum obtained from this voxel. The majority of signals belong to major biliary lipids – chol-PLs, cholesterol and various bile acids. The peaks were assigned based on the *in vitro* studies performed by Ijare *et al.* (10) and Gowda *et al.* (12) and the *in vivo* studies on human (18) and monkey bile (19). The signal at 0.66 ppm, marked as peak 1, was assigned to the $-CH_3$ group of TBAs (H-18 protons). This peak has contributions from cholesterol as well (10,19). Peak 2 at 0.88 ppm was assigned to protons of the ring bound $-CH_3$ group of bile acids (H-19 protons). Peak 3 in the region 0.99 – 1.02 ppm was assigned to the H-21 $-CH_3$ protons of bile acids (12,19). The signal at 1.26 was assigned to the $-CH_2-$ protons of the aliphatic tail of phospholipids (peak 4). A group of overlapping peaks in the region 1.45–2.73 ppm (region 5) represents the remainder of the aliphatic protons in bile acids, chol-PLs and cholesterol (10,19). The $-N^+(CH_3)_3$ group of chol-PLs was observed at 3.22 ppm, peak 7 (10,18,19). The peak at 3.08 ppm (peak 6) was assigned to the H-26 $-CH_2-$ group of TCBAs, whereas the signal at 3.74 ppm was assigned to the H-25 $-CH_2-$ group of GCBAs (peak 8). The olefinic ($-CH=CH-$) protons of chol-PLs resonate at 5.28 ppm, marked as peak 10 (19). Lastly, the broad overlapping peaks (peak 11) resonating in the region 7.76–8.05 ppm were assigned to the amide ($-NH$) groups of both GCBAs and TCBAs (10,19). Panel (E) compares the actual spectrum of human bile *in vivo* (bottom) with its synthesized spectrum obtained by FELIX-2007 software, based on Lorentzian fitting (middle), and the residual spectrum (top).

Out of the 17 spectra obtained from healthy volunteers, 14 were included in the quantification (see Table 1 for details). Peaks of bile metabolites with a known role in HPB disorders (7–11,17,28), and which were resolved in the *in vivo* ^{1}H MR spectrum, were selected for the quantification (i.e. peaks 1, 6, 7, 8, and 11 in panel (D)). Table 4 lists the concentrations (mM) of metabolites quantified after applying T_1, T_2 and CF(H_2O) corrections as discussed in the methods section. The means and standard deviations for TBAs plus cholesterol, TCBAs, GCBAs and chol-PLs were calculated. From Table 4, it is obvious that the mean

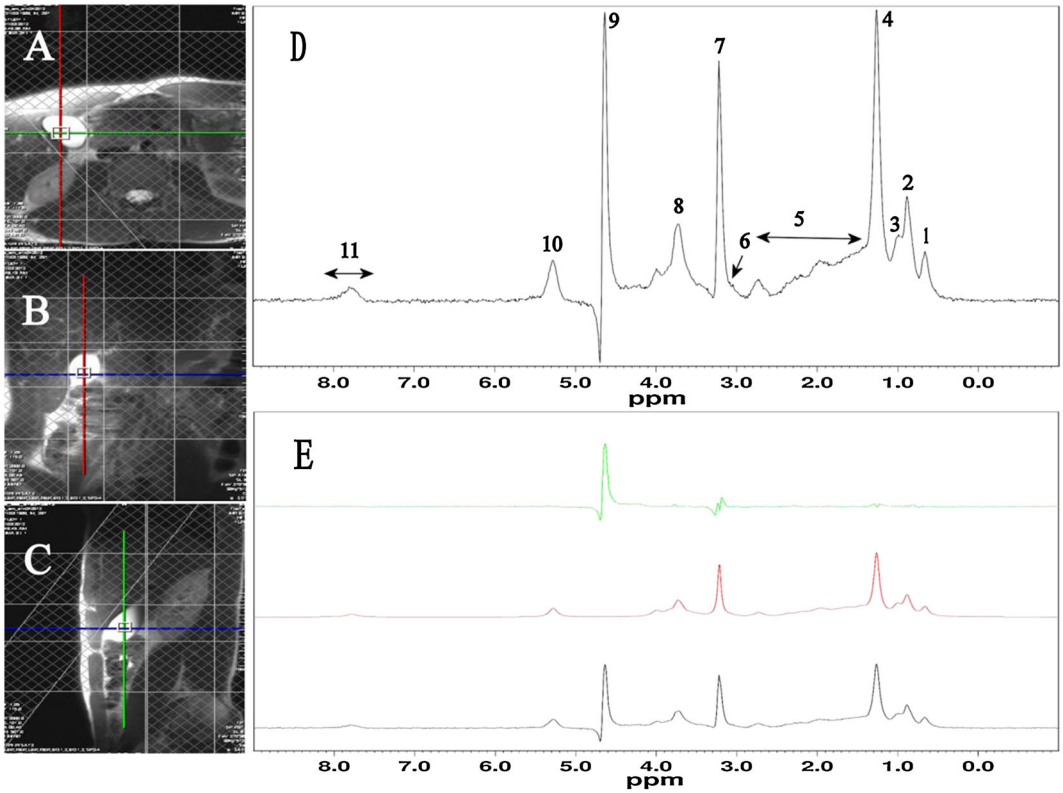

Figure 2. ^{1}H MR spectrum of human gallbladder bile acquired from a healthy volunteer *in vivo* with a 3 T Siemens scanner using a custom-built receive-only coil. (A)–(C) Transverse, coronal and sagittal images acquired at the end of expiration during a regular breath-hold and used for the positioning of a $12 \times 12 \times 12\ mm^3$ voxel in the gallbladder. (D) The corresponding ^{1}H MR spectrum of gallbladder bile obtained from this voxel. The peaks were assigned based on the previous *in vitro* (10,12) and *in vivo* (18,19) studies. *Assignments:* 1, H-18 protons of $-CH_3$ group of TBAs (this peak also has a contribution from cholesterol H-18 protons of the $-CH_3$ group); 2, protons from the ring bound $-CH_3$ group of bile acids (H-19); 3, H-21 $-CH_3$ protons of bile acids; 4, $-CH_2-$ protons of aliphatic tail of chol-PLs; 5, the remainder of the aliphatic protons in bile acids, chol-PLs and cholesterol; 6, H-26 protons of $-CH_2-$ group of TCBAs; 7, $-N^+(CH_3)_3$ group of chol-PLs; 8, H-25 protons of $-CH_2-$ group of GCBAs; 9, residual water; 10, olefinic ($-CH=CH-$) protons of chol-PLs; 11, amide ($-NH$) group of both GCBAs and TCBAs. (E) Comparison of the actual spectrum of human bile *in vivo* (bottom) with its synthesized spectrum (middle); the residual spectrum is shown at the top.

Table 4. Concentrations of metabolites (mM) in healthy volunteers and their means and SDs

Subject	(TBAs + cholesterol) 0.66 ppm	TCBAs 3.08 ppm	chol-PLs 3.22 ppm	GCBAs 3.74 ppm	TBAs (amide group) 7.76–8.05 ppm
1	120.43	56.71	69.90	51.44	102.18
2	NR	NR	69.58	98.88	106.87
3	97.73	15.36	44.64	NR	96.29
4	115.55	50.92	70.97	36.98	108.29
5	186.25	29.32	66.47	78.75	99.50
6	115.21	17.36	31.41	23.79	40.16
7	82.76	NR	25.21	43.68	22.39
8	133.16	16.38	37.75	73.59	83.90
9	72.09	5.83	21.95	12.75	21.32
10	47.58	NR	24.43	28.18	20.61
11	230.24	29.62	79.55	101.51	ND
12	91.28	19.76	36.78	26.03	ND
13	235.15	30.41	58.34	76.13	93.97
14	77.71	11.34	29.08	58.68	72.77
Mean	123.47	25.73	47.58	54.65	72.35
SD	59.09	15.96	20.65	29.21	35.80

NR, not resolved; ND, not detected.

concentrations of all the quantified metabolites were well within the range of biliary biochemicals reported earlier (10,18,29).

Figure 3 shows the 2D L-COSY spectrum of human gallbladder bile obtained *in vivo* from healthy volunteers. This is the first report of an *in vivo* 2D L-COSY spectrum of human gallbladder bile. Figure 3(A) shows a typical *in vivo* 2D spectrum of bile with water suppression band width of 35 Hz and 50 increments, Fig. 3(B) represents a 2D spectrum with water suppression band width of 50 Hz and 50 increments, and Fig. 3(C) shows a 2D spectrum with water suppression band width of 35 Hz and 39 increments. In this case, although 50 measurements were acquired, only the first 39 measurements were processed due to technical issues. All three spectra are linear predicted to 64 increments. The *in vivo* 2D L-COSY spectrum was compared with its *in vitro* counterpart (8,13), and the following assignments were made. The diagonal peak at $F_2 = F_1 = 7.82 \pm 0.04$ ppm, mean ± SD along with a cross peak at $F_2 = 7.80 \pm 0.05$, $F_1 = 3.70 \pm 0.10$ ppm represents the amide group of TCBAs and GCBAs (contours 1, detected in 8/11 cases, and 1a, detected in 6/11 cases). It should be noted that both TCBAs and GCBAs were overlapping compared with the *in vitro* spectra (8). This is due to the use of a lower magnetic field strength (3 T versus 8.5 T) in this study. The diagonal peak at $F_2 = F_1 = 5.29 \pm 0.02$ ppm represents the olefinic (−CH = CH–) protons of chol-PLs (marked as 2, detected in 11/11 cases) along with the cross peaks ($F_2 = 5.29 \pm 0.02$, $F_1 = 2.74 \pm 0.10$ ppm) and ($F_2 = 5.28 \pm 0.04$, $F_1 = 2.00 \pm 0.08$ ppm) representing *J*-coupling of the olefinic protons with neighbouring methylene protons (contours 2a, detected in 10/11 cases, and 2b, detected in 9/11 cases). The diagonal peak at $F_2 = F_1 = 4.24 \pm 0.07$ ppm was assigned to the PC-glyceryl 1-CH_2 protons (marked as 3, detected in 8/11 cases).The glyceryl 2-CH signals of PC appeared as a cross peak ($F_2 = 5.28 \pm 0.04$, $F_1 = 4.25 \pm 0.07$ ppm) with low intensity (marked as 3a, detected in 3/11 cases). Detection of this cross peak in only 3/11 subjects could be attributed to the very low intensity of this cross peak. This cross peak would serve as a marker in detecting the presence/absence of PC in bile and will be valuable in differentiating PC from other chol-PLs (8). The diagonal peak at $F_2 = F_1 = 3.71 \pm 0.03$ ppm was assigned to the PC-cholyl N–CH_2– protons (marked as 4, detected in 11/11 cases), and the symmetric cross peaks at $F_2 = 4.34 \pm 0.05$, $F_1 = 3.68 \pm 0.05$ ppm and $F_2 = 3.66 \pm 0.02$, $F_1 = 4.39 \pm 0.14$ ppm represent *J*-coupling between the –N–CH_2– and –CH_2-O– of chol-PLs (marked as 4a and 4b, detected in 6/11 cases).The diagonal peak at $F_2 = F_1 = 3.21 \pm 0.01$ ppm was assigned to the $-N^+(CH_3)_3$ group of chol-PLs (marked as 5, detected in 11/11 cases). The diagonal peak at $F_2 = F_1 = 3.06 \pm 0.03$ ppm (marked as 6, detected in 11/11 cases) was assigned to the H-26 –CH_2– protons of TCBAs along with the cross peak at $F_2 = 3.60 \pm 0.03$, $F_1 = 3.10 \pm 0.08$ ppm representing coupling between the H-25 and H-26 –CH_2– protons of TCBAs (marked as 6a, detected in 9/11 cases). The diagonal peak at $F_2 = F_1 = 0.68 \pm 0.03$ ppm represents TBAs plus cholesterol (marked as 7, detected in 11/11 cases). It should be noted that the chemical shift values recorded in the 2D spectrum were slightly different from those of the 1D spectrum due to the limited number of data points available in the 2D spectrum in both dimensions.

It should be noted that Fig. 3(B) looks similar to Fig. 3(A) (with some additional noise peaks), showing all the diagonal/cross peaks detected in Fig. 3(A) except for the cross peak 3a. Interestingly, the cross peak marked as 4a ($F_2 = 4.32$ ppm, $F_1 = 3.66$ ppm), which is very close to the water signal, was also observed. This indicates that the increase in the water suppression band-width (from 35 Hz to 50 Hz) has negligible or no effect on the spectral quality. Similarly, the decrease in the number of increments shows negligible effect in the spectral quality (Fig. 3(C)). This shows that the linear prediction from 40 to 64 increments provided similar results to the linear prediction from 51 to 64 increments.

DISCUSSION

MRS can reveal subtle changes in biochemistry (due to its high resolution) following the metabolic alterations in the early stages of disease in a single experiment. This makes MRS an attractive tool in medical diagnosis (29,30). In particular, it is a potential

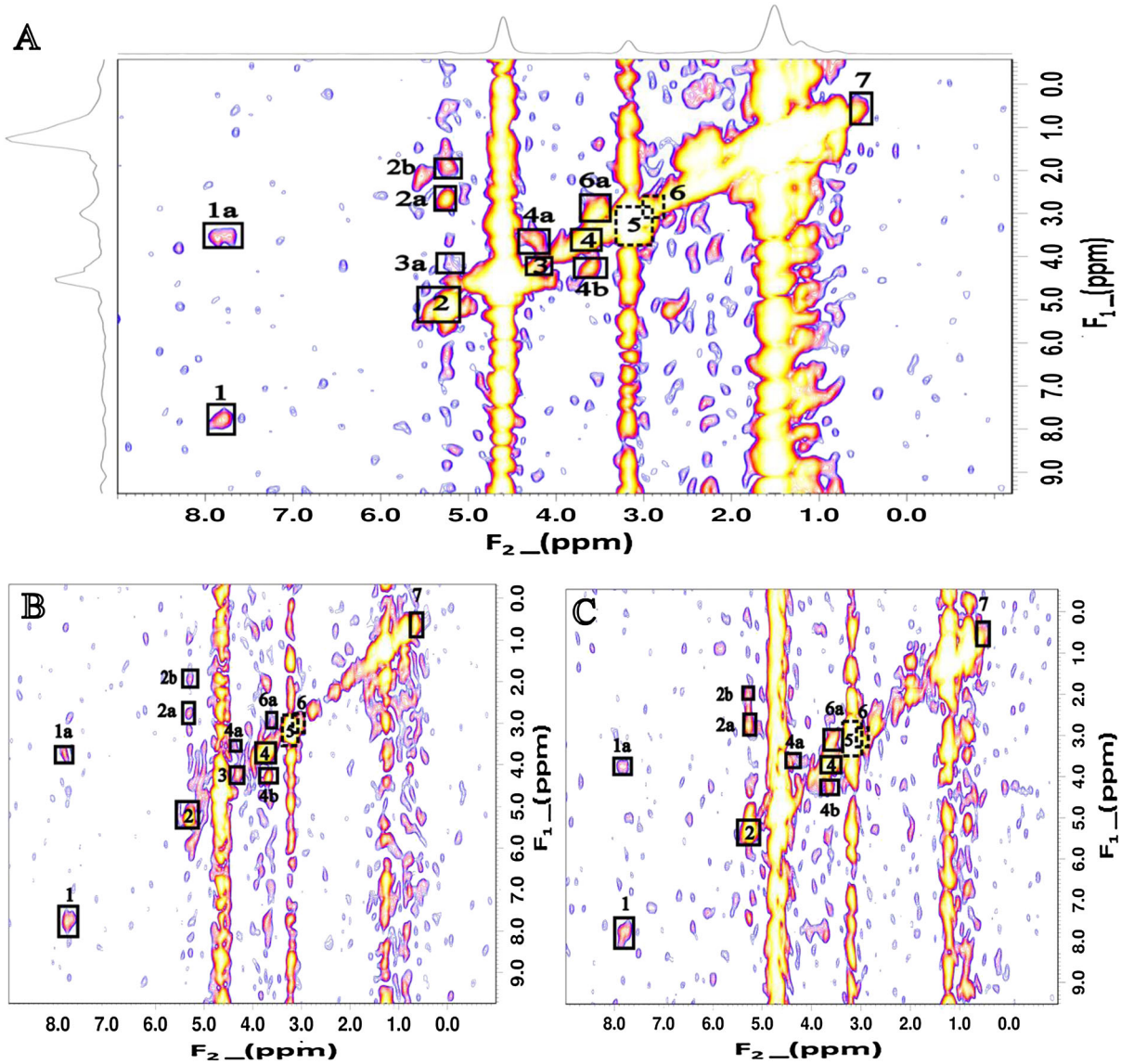

Figure 3. 2D L-COSY spectrum of human gallbladder bile *in vivo* obtained from healthy volunteers. (A) Typical *in vivo* 2D spectrum of bile with water suppression band width of 35 Hz and 50 increments, (B) 2D spectrum with water suppression band width of 50 Hz and 50 increments and (C) 2D spectrum with water suppression band width of 35 Hz and 39 increments. All three spectra are linear predicted to 64 increments. The following diagonal peaks and cross peaks were assigned based on the *in vitro* studies (8,13): 1, 1a, diagonal and cross peaks representing the amide group of TCBAs and GCBAs; 2, 2a, 2b, diagonal peak representing the olefinic (−CH = CH–) protons of chol-PLs and two cross peaks representing *J*-coupling of the olefinic protons with neighbouring methylene protons; 3, 3a, diagonal peak representing PC-glyceryl 1-CH_2 protons and cross peak representing *J*-coupling of the glyceryl 2-CH with 3-CH_2 of PC; 4, 4a, 4b, diagonal peak representing PC-cholyl- N–CH_2– protons and symmetric cross peaks showing *J*-coupling between –N–CH_2– and –CH_2–O– of chol-PLs; 5, diagonal peak representing the $-N^{+}(CH_3)_3$ group of chol-PLs; 6 and 6a, diagonal peak representing the H-26 –CH_2– protons of TCBAs and cross peak representing *J*-coupling between the H-25 and H-26 –CH_2– protons of TCBAs; 7, diagonal peak assigned to TBAs plus cholesterol.

non-invasive tool for differentiating malignant changes from benign disorders (31). In the past, a number of *in vitro* bile MRS studies introduced the value of this technique in the early diagnosis of HPB disorders (3–8,17,28,32). Bile for such studies was collected during invasive procedures such as endoscopic retrograde cholangiopancreatography (ERCP) or surgery. *In vivo* MRS would have enormous potential in the non-invasive analysis of bile. The first attempt by Prescot *et al.* (18) was successful in quantifying only one component of bile, chol-PLs. The spectral quality was low and other components of bile such as GCBAs and TCBAs, which have a major role in the pathophysiology of HPB diseases, were not quantified. This could be due to the low magnetic field strength, the use of spin echoes with long delays, magnetic susceptibilities, motion of the gallbladder, especially due to breathing, and/or lipid contamination. In the second attempt, Künnecke *et al.* obtained a good quality *in vivo* ^{1}H MR spectrum of gallbladder bile from cynomolgus monkeys using a 4.7 T animal scanner with the aid of a transmit/receive surface coil (19). However, the 4.7 T scanner and transmit/receive surface coils are not routine for clinical use. The current study showed the feasibility of acquiring a good quality ^{1}H MR spectrum under current clinical settings (3 T scanner and receive surface array coils).

To overcome some of the limitations of the previous study in humans (18), we employed a field strength of 3 T, and decreased T_E from 60 to 30 ms, which can significantly reduce the T_2 loss. Moreover, we used a bellow respiratory-gated sequence to reduce the motion artifacts due to breathing. With these improvements, we were able to quantify other major lipid components of bile – TBAs plus cholesterol, TCBAs and GCBAs, including the previously reported chol-PLs (18). The peak resonating at 0.66 ppm has contributions from the H-18 methyl protons of TBAs and cholesterol. However, earlier *in vitro* studies have revealed that the percentage of cholesterol contributing to this signal is very low. As a result, the peak mostly represents the sum of TCBAs and GCBAs (10). This fact could partially be explained by the lower mobility of cholesterol molecules due to their participation in phospholipid membranes. This results in loss of cholesterol signals due to shorter T_2 relaxation time (33). However, in the current study, the concentration of TBAs + cholesterol quantified from the 0.66 ppm peak was 123.47 ± 59.09 mM (mean ± SD), which is higher than in the previous *in vitro* studies (TBAs + cholesterol 72.76 ± 55.06 mM, mean ± SD, as reported by Gowda *et al.* (29)). However, most of the individual values (except in three cases, Table 4) fall in the range 0.38–178.61 mM, as reported by Gowda *et al.* (29). In the majority of *in vitro* studies, the samples were collected from participants who were suffering from some sort of HPB disorder, the major reason for ERCP to be performed. As a result, the concentrations determined in *in vitro* studies may reasonably be expected to differ from our *in vivo* results gathered non-invasively from healthy volunteers, without any medical interference and use of radiopaque agents.

Given that the TBA pool in the bile is almost completely conjugated to glycine and/or taurine, and under the conditions of low biliary cholesterol, the levels of lipids determined from the 0.66 ppm peak should be comparable to the sum of TCBAs and GCBAs (10). However, in the current study, the mean concentration of lipids calculated from the 0.66 ppm peak is 53% higher than the mean of the sum of GCBAs and TCBAs (as opposed to the 10% expected) due to contamination from cholesterol (19,34). Surprisingly, the study by Künnecke *et al.* (19) on the gallbladder bile of monkeys revealed even higher concentrations of lipids in this region (267 ± 47 mM; mean ± SD). One explanation could be the effect of lipid contamination by body fat surrounding the gallbladder in *in vivo* studies. Although we used spatial saturation bands around the gallbladder to suppress the contribution from outside fat, it is difficult to remove such effects completely. Despite the use of respiratory-gated sequences, a residual breathing motion artifact may also contribute to the apparent lipid contamination.

Since a majority of bile acids in bile are conjugated to glycine and/or taurine, Ijare *et al.* explored the use of the amide protons of conjugated bile acids (resonating in the region 7.80–8.10 ppm) to quantify the sum of GCBAs and TCBAs for *in vitro* applications (13). However, the amide protons are in dynamic exchange with biliary water at physiologic pH (7.0–7.7) (35), and do not represent the true signal intensity. As a result, one of the prerequisites for using such a methodology was to adjust the pH of bile to a value slightly lower than the physiologic pH (6 ± 0.5). In *in vivo* studies such manipulation of pH is not possible; however, the pH of bile is generally decreased during its concentration in the gallbladder (36). This could be an advantage for *in vivo* studies. We mostly recruited subjects who had fasted overnight or for at least four hours in order to have a gallbladder that was completely filled with bile. Therefore, the pH of bile should not affect the signal intensity of amide protons in the bile concentrated after overnight fasting. Based on Table 4, in most cases the concentrations of GCBAs and TCBAs calculated from the amide region are slightly less than the sums of concentrations calculated from 3.74 and 3.08 peaks. In two cases the signal from the amide region was not detected. This could be due to the very high pH of the bile. However, in three cases the concentrations of GCBAs and TCBAs calculated from the amide region were slightly more than the sums of concentrations of GCBAs and TCBAs calculated from 3.74 and 3.08 peaks. Considering the breadth of the amide region, there could be a random error in measuring the area under these peaks.

A more accurate method of quantifying TCBAs and GCBAs is to use their $-CH_2-$ peaks resonating at 3.08 and 3.74 ppm, respectively (10). This approach is independent of the pH effect. Moreover, these peaks are not affected by lipid contamination. Since the ratio of GCBAs/TCBAs plays an important role in HPB disorders (10), determining this ratio may be valuable in the diagnosis of HPB diseases. In this study, the mean of the GCBA/TCBA ratio was 2.48 (2.48 ± 1.51, mean ± SD), which is very close to the expected value, 3 (37). However, there were cases in which this ratio was even less than unity. Given the small sample size, it is difficult to draw a rigorous conclusion in this study. The chol-PLs were quantified from the signal resonating at 3.22 ppm following a strategy similar to that of Prescot *et al.* (18). The levels of chol-PLs determined in this study (47.58 ± 20.65 mM, mean ± SD) were comparable to those reported earlier (35.8 ± 9.8 mM, mean ± SD) (18).

As presented in Table 4, there was a considerable variability in the concentration of biliary metabolites, which may raise concerns regarding the diagnostic value of these metabolites. Such variability was reported in previous *in vitro* (29) and *in vivo* (18) studies as well. As explained by Khan *et al.* (17), the concentration of bile metabolites varies between subjects and within a subject over time. This is primarily due to variations in diet, nutritional status, drugs and environmental exposure. In an *in vitro* study by Albiin *et al.* (7), although there were similar variabilities, the differences between normalized intensities of PC and TCBAs in non-cancer and cancer patients were statistically significant. In this study, although there is a considerable variability in the concentrations of bile metabolites, the quantification of these metabolites is still useful and can be used for the differentiation of various HPB disorders.

Considering that age, sex, variation in diet, and exposure to xenobiotics are partly responsible for the variation in the concentrations of biliary metabolites (17,19), eliminating such confounding factors may help decrease the variability. In the study by Künnecke *et al.* (19), the researchers selected male monkeys with similar ages and put them on a similar diet. This reduced the SD in the TBA measurements to less than 20% of the mean. Based on this study, one can infer that the biliary metabolites represent the individual's metabolism, and if we follow the bile composition in the same patient over time we may be able to follow up the progress of the disease, which can be quite useful in the clinic.

1D spectra cannot provide complete information regarding the metabolite composition of the bile. Furthermore, signals arising from some of the bile metabolites important in HPB pathologies, such as lactate and the glyceryl region of PC, overlap with lipid signals (8). Moreover, some important regions such as the amide region have a very low intensity in the 1D spectrum

and are not detectable in some subjects. In order to detect such signals separately, 2D L-COSY spectra (15,16) were obtained for the first time from human gallbladder bile *in vivo*. A cross peak from the PC-glyceryl signals ($F_2 = 5.28 \pm 0.04$, $F_1 = 4.25 \pm 0.07$ ppm) has been detected in the L-COSY spectrum, which overlapped the lipid signal in the corresponding 1D spectrum. Detection of these signals may be helpful in the diagnosis of HPB pathologies (8).

This was the first attempt to obtain 2D spectra from the gallbladder *in vivo*, which is a moving organ. Although we were able to detect and assign some cross peaks with clinical importance based on their chemical shifts observed *in vitro*, the quantification was not reliable due to high levels of noise. The quality of the 2D spectra should be improved further by increasing signal-to-noise ratio (using higher magnetic field strength and better RF coils), decreasing echo time and decreasing t_1 noise in order to achieve a reliable volume measurement of cross peaks. Therefore, in this study, we are presenting the first 2D L-COSY spectra from bile inside the gallbladder only qualitatively.

CONCLUSIONS

This study showed the possibility of obtaining good quality 1D ^{1}H MR spectra of gallbladder bile *in vivo* using a 3 T clinical scanner. It facilitated the simultaneous quantification of TBAs plus cholesterol, TCBAs, and GCBAs, including the previously reported chol-PLs, which have a major role in the pathophysiology of HPB diseases. This approach may be helpful in the early non-invasive diagnosis of HPB disorders. Detection of PC-glyceryl signals in the L-COSY spectrum, which overlapped with the lipid signal in the corresponding 1D spectrum, can prove the value of 2D techniques in the differentiation of PC from its hydrolysis products such as lysophosphatidylcholine and phosphorylcholine, which are detrimental to the HPB system. Moreover, 2D techniques can augment the diagnostic accuracy of 1D methods. However, 2D techniques are time consuming and warrant further development in order to improve the spectral quality and reduce scanning time.

REFERENCES

1. Sherwood L. The digestive system. In: *Human Physiology: From Cells to Systems*, Alexander S, Glubka A, Crosby L, Oliveira L (eds). Brooks/Cole Cengage Learning: Belmont, CA, 2013, 581–634.
2. Silverthorn DU. The digestive system. In: *Human Physiology: an Integrated Approach*, Volker KK, Scanlan-Rohrer A, Reid AA, Williams A, Cogan D, Tabor N, Padial A (eds). Pearson Education: Boston, MA, 2012, 696–735.
3. Gowda GA. NMR spectroscopy for discovery and quantitation of biomarkers of disease in human bile. Bioanalysis 2011; 3: 1877–1890.
4. Gowda GA. Human bile as a rich source of biomarkers for hepatopancreatobiliary cancers. Biomark. Med. 2010; 4: 299–314.
5. Hofmann AF. The continuing importance of bile acids in liver and intestinal disease. Arch. Intern. Med. 1999; 159: 2647–2658.
6. Bezabeh T, Ijare OB, Albiin N, Arnelo U, Lindberg B, Smith ICP. Detection and quantification of D-glucuronic acid in human bile using ^{1}H NMR spectroscopy: relevance to the diagnosis of pancreatic cancer. Magn. Reson. Mater. Phys., Biol. Med. 2009; 22: 267–275.
7. Albiin N, Smith ICP, Arnelo U, Lindberg B, Bergquist A, Dolenko B, Bryksina N, Bezabeh T. Detection of cholangiocarcinoma with magnetic resonance spectroscopy of bile in patients with and without primary sclerosing cholangitis. Acta Radiol. 2008; 49: 855–862.
8. Ijare OB, Bezabeh T, Albiin N, Arnelo U, Bergquist A, Lindberg B, Smith ICP. Absence of glycochenodeoxycholic acid (GCDCA) in human bile is an indication of cholestasis: a ^{1}H MRS study. NMR Biomed. 2009; 22: 471–479.
9. Nagana Gowda GA, Shanaiah N, Cooper A, Maluccio M, Raftery D. Visualization of bile homeostasis using ^{1}H-NMR spectroscopy as a route for assessing liver cancer. Lipids 2009; 44: 27–35.
10. Ijare OB, Bezabeh T, Albiin N, Bergquist A, Arnelo U, Lindberg B, Smith ICP. Simultaneous quantification of glycine- and taurine-conjugated bile acids, total bile acids, and choline-containing phospholipids in human bile using ^{1}H NMR spectroscopy. J. Pharm. Biomed. Anal. 2010; 53: 667–673.
11. Bezabeh T, Ijare OB, Albiin N, Bergquist A, Arnelo U, Löhr M, Hov JR, Smith ICP. Alteration in the conjugation pattern of bile acids in human bile during cholestasis: a ^{1}H MRS study. Proc. Int. Soc. Magn. Reson. Med. 2010; 18: 4590.
12. Gowda GA, Ijare OB, Somashekar BS, Sharma A, Kapoor VK, Khetrapal CL. Single step analysis of individual conjugated bile acids in human bile using ^{1}H NMR spectroscopy. Lipids 2006; 41: 591–603.
13. Ijare OB, Somashekar BS, Gowda GA, Sharma A, Kapoor VK, Khetrapal CL. Quantification of glycine and taurine conjugated bile acids in human bile using ^{1}H NMR spectroscopy. Magn. Reson. Med. 2005; 53: 1441–1446.
14. Rothman DL, Behar KL, Hetherington HP, Shulman RG. Homonuclear ^{1}H double-resonance difference spectroscopy of the rat brain in vivo. Proc. Natl. Acad. Sci. U. S. A. 1984; 81: 6330–6334.
15. Thomas MA, Yue K, Binesh N, Davanzo P, Kumar A, Siegel B, Frye M, Curran J, Lufkin R, Martin P, Guze B. Localized two-dimensional shift-correlated MR spectroscopy of human brain. Magn. Reson. Med. 2001; 46: 58–67.
16. Thomas MA, Hattori N, Umeda M, Sawada T, Naruse S. Evaluation of two-dimensional L-COSY and JPRESS using a 3 T MRI scanner: from phantoms to human brain *in vivo*. NMR Biomed. 2003; 16: 245–251.
17. Khan SA, Cox IJ, Hamilton G, Thomas HC, Taylor-Robinson SD. *In vivo* and *in vitro* nuclear magnetic resonance spectroscopy as a tool for investigating hepatobiliary disease: a review of H and P MRS applications. Liver Int. 2005; 25: 273–281.
18. Prescot AP, Collins DJ, Leach MO, Dzik-Jurasz AS. Human gallbladder bile: noninvasive investigation *in vivo* with single-voxel ^{1}H MR spectroscopy. Radiology 2003; 229: 587–592.
19. Künnecke B, Bruns A, von Kienlin M. Non-invasive analysis of gallbladder bile composition in cynomolgus monkeys using *in vivo* ^{1}H magnetic resonance spectroscopy. Biochim. Biophys. Acta 2007; 1771: 544–549.
20. Mohajeri S, Bezabeh T, King SB, Ijare OB, Minuk GY, Lipschitz J, and Smith ICP. *In vivo* ^{1}H MRS of gallbladder bile using an optimized 8-channel phased array at 3 T: towards improved diagnosis of hepatopancreatobiliary diseases. Proc. Int. Soc. Magn. Reson. Med. 2010; 18: 4595.
21. Ijare OB, Smith ICP, Mohajeri S, Bezabeh T. Magnetic resonance spectroscopy of bile in the diagnosis of hepatopancreaticobiliary diseases: past, presence and future. In: *Future Directions of NMR*, Khetrapal CL, Kumar A, Ramanathan KV (eds). Springer: New Delhi, 2011, 45–53.
22. Provencher S. Making the basis set. In: *LCModel & LCMgui User's Manual*. LCMODEL: Oakville, Ontario, 2013, 79–102. http://lcmodel.ca/pub/LCModel/manual/manual.pdf [2 December 2013].
23. Klose U. *In vivo* proton spectroscopy in presence of eddy currents. Magn. Reson. Med. 1990; 14: 26–30.
24. Roemer PB, Edelstein WA, Hayes CE, Souza SP, Mueller OM. The NMR phased array. Magn. Reson. Med. 1990; 16: 192–225.
25. Fayad LM, Salibi N, Wang X, Machado AJ, Jacobs MA, Bluemke DA, Barker PB. Quantification of muscle choline concentrations by proton MR spectroscopy at 3 T: technical feasibility. Am. J. Roentgenol. 2010; 194: W73–79.
26. van Erpecum KJ. Biliary lipids, water and cholesterol gallstones. Biol. Cell 2005; 97: 815–822.
27. Bolan PJ, Meisamy S, Baker EH, Lin J, Emory T, Nelson M, Everson LI, Yee D, Garwood M. *In vivo* quantification of choline compounds in the breast with ^{1}H MR spectroscopy. Magn. Reson. Med. 2003; 50: 1134–1143.
28. Cox IJ, Sharif A, Cobbold JF, Thomas HC, Taylor-Robinson SD. Current and future applications of *in vitro* magnetic resonance spectroscopy in hepatobiliary disease. World J. Gastroenterol. 2006; 12: 4773–4783.
29. Gowda GA, Somashekar BS, Ijare OB, Sharma A, Kapoor VK, Khetrapal CL. One-step analysis of major bile components in human bile using ^{1}H NMR spectroscopy. Lipids 2006; 41: 577–589.
30. Smith ICP, Baert R. Medical diagnosis by high resolution NMR of human specimens. IUBMB Life 2003; 55: 273–277.

31. Mountford C, Smith ICP, Bourne R. Correlation of histopathology with magnetic resonance spectroscopy of human biopsies. In: *Modern Magnetic Resonance*, Vol. II, Webb GA (ed.). Springer: London, 2006, 1027–1036.
32. Nishijima T, Nishina M, Fujiwara K. Measurement of lactate levels in serum and bile using proton nuclear magnetic resonance in patients with hepatobiliary diseases: its utility in detection of malignancies. Jpn. J. Clin. Oncol. 1997; 27: 13–17.
33. Ellul JP, Murphy GM, Parkes HG, Slapa RZ, Dowling RH. Nuclear magnetic resonance spectroscopy to determine the micellar cholesterol in human bile. FEBS Lett. 1992; 300: 30–32.
34. Stephan ZF, Armstrong MJ, Hayes KC. Bile lipid alterations in taurine depleted monkeys. Am. J. Clin. Nutr. 1981; 34: 204–210.
35. Murray RK, Granner DK, Mayes PA, Rodwell VM. *Harper's Biochemistry*. Prentice-Hall: Norwalk CT, 1988, 580.
36. Marteau C, Sastre B, Iconomidis N, Portugal H, Pauli AM, Gérolami A. pH regulation in human gallbladder bile: study in patients with and without gallstones. Hepatology 1990; 11: 997–1002.
37. Bove KE, Heubi JE, Balistreri WF, Setchell KD. Bile acid synthetic defects and liver disease: a comprehensive review. Pediatr. Dev. Pathol. 2004; 7: 315–334.